Enhancing monochromatic multipole emission by a subwavelength enclosure of degenerate Mie resonances

Jiajun Zhao, Likun Zhang, and Ying Wu

Citation: The Journal of the Acoustical Society of America **142**, EL24 (2017); doi: 10.1121/1.4990010
View online: http://dx.doi.org/10.1121/1.4990010
View Table of Contents: http://asa.scitation.org/toc/jas/142/1
Published by the Acoustical Society of America

Enhancing monochromatic multipole emission by a subwavelength enclosure of degenerate Mie resonances

Jiajun Zhao,[1,a)] Likun Zhang,[2] and Ying Wu[1]
[1]*King Abdullah University of Science and Technology (KAUST), Division of Computer, Electrical and Mathematical Science and Engineering, Thuwal, 23955-6900, Saudi Arabia*
[2]*National Center for Physical Acoustics and Department of Physics and Astronomy, University of Mississippi, University, Mississippi 38677, USA*
zhaojiajun1990@gmail.com; zhang@olemiss.edu; ying.wu@kaust.edu.sa

Abstract: Sound emission is inefficient at low frequencies as limited by source size. This letter presents enhancing emission of monochromatic monopole and multipole sources by enclosing the source with a subwavelength circular enclosure filled of an anisotropic material of a low radial sound speed. The anisotropy is associated with an infinite tangential density along the azimuth. Numerical simulations show that emission gain is produced at frequencies surrounding degenerate Mie resonant frequencies of the enclosure, and meanwhile the radiation directivity pattern is well preserved. The degeneracy is theoretically analyzed. A realization of the material is suggested by using a space-coiling structure.

© 2017 Acoustical Society of America
[CCC]
Date Received: March 17, 2017 **Date Accepted:** June 13, 2017

1. Introduction

Sound emission rate at low frequencies is extremely low because of the smallness of the source size relative to the large wavelength of low-frequency sound ($D < \lambda$). The sound power radiated to far field by a monopole source is proportional to $(kD)^2$ ($k = 2\pi/\lambda$ is wavelength), and the power decreases proportionally for higher multipoles.[1] This present study proposes to enclose monochromatic multipole sources of different orders (including monopole) in a deep subwavelength structure (e.g., $D \ll \lambda$) that can eventually enhance the source emission and meanwhile preserve the directivity pattern of the emitted sound waves.

Existing methods enhancing sound source emission somehow alters the directivity pattern of the emitted sound. A loudspeaker mouth adapted in a horn shape improves the emission but confines the radiation in limited space.[2,3] A woofer diaphragm is mounted in a speaker cabinet to boost the low-frequency emission, but the emission is not omnidirectional, and additionally, there are requirements on damping sounds that get into walls of the cabinet.[4] Recently, acoustic slab metamaterials were used to enhance emission of a *monopole* source in a subwavelength space, but the employed Fabry-Pérot resonances between two planar structures inevitably alter the omnidirectional radiation directivity.[5]

This present work enhances emission of monopole and multipole sources without altering the directivity by enclosing the source in a subwavelength circular structure of an *anisotropic* material of *degenerate* Mie resonances. The anisotropy is associated with an infinite tangential density along the azimuthal direction. Numerical simulations of both monopole and multipole sources enclosed by the material show emission gain at frequencies surrounding Mie resonant frequencies of the material (Sec. 2). Enhancing emission of higher multipoles would otherwise be impossible by a subwavelength *isotropic* material of common Mie resonances whose resonant frequencies increase for higher multipoles. The *anisotropic* material presented here has the ability to degenerate the resonant frequencies of higher multipoles to the same frequency as dipole, as analyzed in Sec. 3, consequently enabling emission gain of higher multipoles by the subwavelength enclosure. A space-coiling structure is implemented to realize the anisotropic material for emission enhancement in practice (Sec. 4).

2. Omnidirectional enhancement of monopole and multipole emission

This section presents simulations of the emission enhancement by an conceptual enclosure of a subwavelength diameter $D < \lambda$, illustrated in Fig. 1(a) as a circular annulus

[a)]Also at: National Center for Physical Acoustics and Department of Physics and Astronomy, University of Mississippi, University, MS 38677, USA.

 © 2017 Acoustical Society of America

(yellow). The enclosure has a constant radial sound speed c_r much smaller than the sound speed in air, c_{air}, and an extremely high density $\rho_\theta \to \infty$ along the azimuthal direction. The low c_r enables the enhancement to occur at low frequencies, while the infinite ρ_θ forces the enhancement of higher multipoles to degenerate at a same low frequency, as we will explain in Sec. 3.

We simulate the emission in two dimensions using COMSOL (acoustic pressure module).[6] A monochromatic monopole source of diameter $0.01D$ is centered in the enclosure and emits sound waves in air. The monopole source is simulated with a constant source strength, i.e., a constant volume flow rate of the source, which is a universal model in reality.[7,8] The anisotropy of the enclosure is simulated with a large number of laminated isotropic layers along the azimuthal direction.

The enhancement is illustrated in Figs. 1(a) and 1(b) by the contrast of sound fields emitted by a monopole source in free space and enclosed by the enclosure. The omnidirectional radiation pattern is clearly unchanged. We characterize the enhancement by the ratio of radiated sound power P_1 in the presence of the enclosure to the power P_0 radiated in free space. The powers are calculated from the far field. The P_1/P_0 values are 76 and 294 for the cases in Figs. 1(a) and 1(b), where the enclosure has a subwavelength dimension of $D = 0.19\lambda$ and 0.14λ, respectively. The results Figs. 1(a) and 1(b) are for two enclosures of the same c_r but different radial density ρ_r (see Fig. 1).

The P_1/P_0 value is further shown in Fig. 1(c) as a function of D/λ. The result is for the enclosure in Fig. 1(b), revealing that the emission gain $P_1/P_0 \geq 1$ is produced at the range of $D/\lambda = [0.01, 0.22]$, $[0.37, 0.49]$, and $[0.68, 0.77]$. The gain surrounds three maxima of Mie resonant frequencies: $P_1/P_0 = 294$, 60, 33 at $D/\lambda = 0.14$, 0.43, 0.73, respectively. The phase distribution of sound fields in the enclosure [insets in Fig. 1(c)] shows a pattern of the monopole Mie resonance.

Numerical results for a dipole source centered in the same enclosure in Fig. 1(b) also show three peak values $P_1/P_0 = 397$, 135, 86 in the subwavelength regime of $D/\lambda = 0.29$, 0.58, 0.87, respectively. The results are shown in Fig. 2(a) where the insets show the pattern of the lowest three dipole Mie resonances corresponding to the three P_1/P_0 peaks. The emisssion gain is produced at the whole range of $D/\lambda = [0.17, 0.97]$. Here the dipole source is simulated in COMSOL by a constant dipole source strength of a diameter $0.01D$.

The enhancement can be understood as the improvement of radiation efficiency, following from the interaction of the enclosure with the near field. Without the enclosure, the majority of emitted low-frequency energy is stored as near-field oscillation rather than radiated to the ambient medium. The storage of sound energy in the near field is a result of the large radiation reactance, which is irrelevant to sound dissipation. The enclosure modifies the source's environment to convert sound energy stored in near fields to that radiated to far fields.

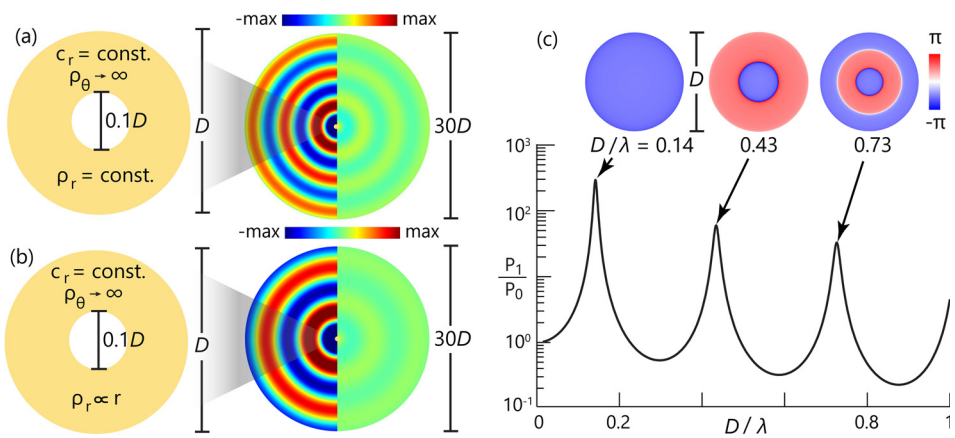

Fig. 1. (Color online) Emission enhancement of a monochromatic monopole source (wavelength λ and diameter $0.01D$) by a circular enclosure of an outer and inner diameter D and $0.1D$ (not scaled in ratio for clear illustration). (a) A contrast of emitted sound fields ($\lambda = 5.26D$) simulated with and without an enclosure (left half vs right half) of a radial density $\rho_r = 14.13\rho_{\text{air}}$ ($\rho_{\text{air}} = 1.21$ kg/m^3). (b) Same as (a) but for $\lambda = 7.14D$ and $\rho_r = 25\pi\rho_{\text{air}}r/D$. (c) The ratio of the radiated power calculated from simulations with and without the enclosure in (b) as a function of D/λ, illustrating emission enhancement surrounding three Mie resonances; the resonances are shown by the phase distribution of sound fields (insets). The simulated enclosures have a small radial sound speed $c_r = 0.266c_{\text{air}}$ ($c_{\text{air}} = 343$ m/s) to enable resonances at low frequencies ($D/\lambda < 1$).

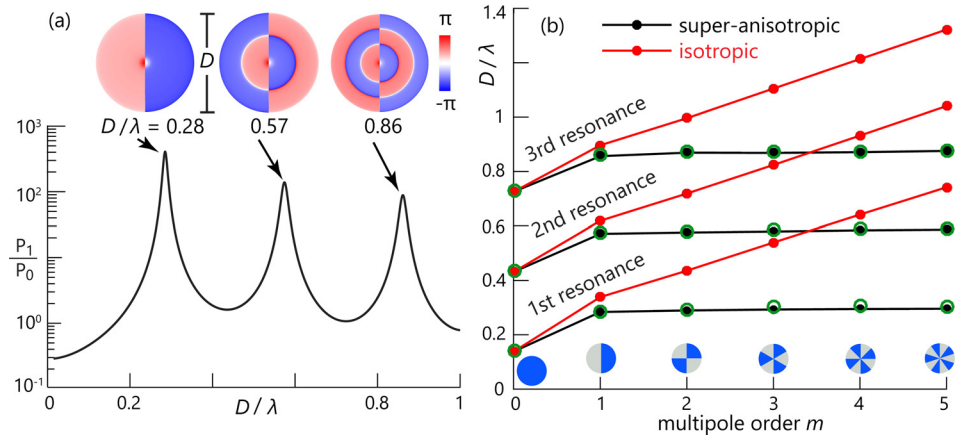

Fig. 2. (Color online) Emission enhancement of monochromatic multipole sources using the enclosure in Fig. 1(b) that has an infinite azimuthal density $\rho_\theta \to \infty$ (i.e., an extreme anisotropy) to degenerate resonant frequencies of higher multipoles. (a) Results as in Fig. 1(c) but for a dipole source also show three resonant peaks at low frequencies ($D/\lambda < 1$). (b) Theoretical calculations of the three D/λ values for higher multipoles show a degeneracy for different multipole orders $m \geq 1$ (black dots), in contrast to an increase with m for an isotropic enclosure of $\rho_\theta = \rho_r$ (red dots). The green circles are simulated results for a realistic structure presented in Fig. 3(a).

3. Analysis of degenerate Mie resonances of the anisotropic material

This section analyzes how the extreme anisotropy ($\rho_\theta \to \infty$) of the material enables the degeneracy of the Mie resonant frequencies of multipole sources of different orders $m =$ integer (with an azimuthal dependence $e^{im\theta}$).

We write the acoustic pressure fields in the enclosure region as $p = R(r)(Ae^{im\theta} + Be^{-im\theta})e^{-i\omega t}$ where $D_I/2 \leq r \leq D/2$ (D_I is the inner diameter of the enclosure). The radial function $R(r)$ subjects to

$$\frac{\rho_r}{r}\frac{d}{dr}\left(\frac{r}{\rho_r}\frac{dR}{dr}\right) + \left(\frac{\omega^2}{c_r^2} - \frac{\rho_r m^2}{\rho_\theta r^2}\right)R = 0, \tag{1}$$

which is derived from the wave equation $\nabla \cdot [(\overline{\overline{\rho}})^{-1}\nabla p] + (\omega^2/B)p = 0$ of an anisotropic medium with $\overline{\overline{\rho}}$ being its mass density tensor and B bulk modulus. Equation (1) explicitly shows that an infinite ρ_θ decouples the multipole order m from $R(r)$, and further indicates that ω is scaled by the radial sound speed c_r of the enclosure. Our enclosure has a small c_r, enabling the emission enhancement to systematically occur at low frequencies for both monopole ($m = 0$) and multipole ($m \neq 0$) sources.

The solutions of Eq. (1) for $\rho_r =$ constant are analytically obtained as

$$p = \left\{ \begin{matrix} J_v(\omega r/c_r) \\ H_v^{(1)}(\omega r/c_r) \end{matrix} \right\} \left\{ \begin{matrix} e^{im\theta} \\ e^{-im\theta} \end{matrix} \right\} e^{-i\omega t}, \quad v = m\sqrt{\frac{\rho_r}{\rho_\theta}}, \tag{2}$$

where $\{\}$ means linear combination, and $J_v(\cdot)$ and $H_v^{(1)}(\cdot)$ are the Bessel and first-kind Hankel functions of order v. The v is forced to be zero by the extreme anisotropy $\rho_\theta \to \infty$, and thus the radial functions are $J_0(\cdot)$ and $H_0^{(1)}(\cdot)$ for multipoles of arbitrary order m.

The resonant frequencies for an enclosure of an inhomogeneous density $\rho_r(r)$ in general, like the one in Fig. 1(b) with $\rho_r = 25\pi\rho_{\text{air}}r/D$, are determined by discretizing the enclosure into N homogeneous rings of different radial density $\rho_r^{(i)} = \rho_r(r_i)$ ($i = 1, 2, ..., N$) and applying the solution Eq. (2) to each layer. The radial components of sound fields follow as

$$R_0(r) = aJ_m(\omega r/c_{\text{air}}) \quad \text{for} \quad r \leq r_0 \equiv D_I/2, \tag{3a}$$

$$R_i(r) = b_i H_0^1(\omega r/c_r) + c_i J_0(\omega r/c_r) \quad \text{for} \quad r_{i-1} \leq r \leq r_i \ (1 \leq i \leq N), \tag{3b}$$

$$R_{N+1}(r) = dH_m^1(\omega r/c_{\text{air}}) + J_m(\omega r/c_{\text{air}}) \quad \text{for} \quad r \geq r_N \equiv D/2, \tag{3c}$$

where the $2(N+1)$ unknown coefficients (a, b_i, c_i, d) and unknown resonant frequencies form an eigen-value problem. It is solved by scattering matrices formed from matching acoustic pressure and velocity at interfaces: $R_i(r) = R_{i+1}(r)$ and [1/

$\rho_r^{(i)}][dR_i(r)/dr] = [1/\rho_r^{(i+1)}][dR_{i+1}(r)/dr]$ at $r = r_i$ $(i = 0, 1, 2, ..., N;\ \rho_r^{(0)} = \rho_r^{(N+1)} \equiv \rho_{\text{air}})$. Calculations with $N = 1$ can give results of an enclosure of a constant density, like the one in Fig. 1(a). For the enclosure in Fig. 1(b) of an inhomogeneous density, the resonant frequencies are calculated with $N = 20$ that gives convergent solutions.

The D/λ values calculated for the enclosure in Fig. 1(b) are shown in Fig. 2(b) by black dots for the lowest three resonances for multipole sources of different orders. The resonances for higher multipoles all occurs in the subwavelength region $D/\lambda < 1$ as in the cases of a monopole ($m = 0$) and dipole ($m = 1$). The frequencies for multipoles of different orders ($m \neq 0$) are degenerate at the same frequency as predicted. There is a frequency difference between the cases of a monopole $m = 0$ and multipoles $m \neq 0$. The difference is due to a contrast of acoustic fields in the inner region $r < D_I/2$ where $J_{m=0}(kr \ll 1) \to 1$ for a monopole source but $J_{m\neq 0}(kr \ll 1) \to 0$ for a multipole source.

The degeneracy of the Mie resonant frequencies presented here differs from the common Mie resonances in an isotropic enclosure, whose resonant frequencies monotonically increase with multipole order m [red dots in Fig. 2(b)]. The degenerate Mie resonances enables simultaneous enhancement of multipole modes of a monochromatic source.

4. Realization of the anisotropic material by a space-coiling structure

This section presents the implementation of a practical structure to realize the conceptual enclosure in Fig. 1(b). The structure is shown in Fig. 3(a) which has outer and inner diameters (D and $D_I = 0.1D$) that are same as the conceptual enclosure. The structure can be made of materials, e.g., brass (gray part), which are rigid enough for a stark contrast of acoustic impedance to the filled air (white part). The air-filled channels of the structure elongate the "acoustic path" (red line) to support the low value of c_r, while the rigid walls that separate the channels support the anisotropy of an extremely high ρ_θ. Such a structure of space-coiling configuration by some modifications has other applications such as for reduced sound transmission[9] and directivity sensing,[10] where the anisotropic feature was not modeled though.

The effective parameters (c_r, ρ_r, ρ_θ) of the structure [cf. Fig. 3(a)] depend on geometrical parameters D_I, D, channel number M, channel width w, and sound path length L of an individual channel. We derive this dependence as

$$c_r = \frac{(D - D_I)c_{\text{air}}}{2L}, \quad \rho_r = \frac{4\pi L \rho_{\text{air}} r}{Mw(D - D_I)}, \quad \rho_\theta \to \infty,\ D_I/2 \le r \le D/2. \tag{4}$$

Briefly, c_r is derived from the conservation of the sound traveling time along the radial direction, $(D - D_I)/2c_r = L/c_{\text{air}}$; ρ_r is derived from the impedance matching condition, i.e., $c_r\rho_r$ equals $c_{\text{air}}\rho_{\text{air}}$ scaled by the structure's air-to-brass filling ratio that varies along r. We use 10 channels ($M = 10$) to maintain reasonable resolutions along the azimuth (as we will illustrate), though the choice is not unique. Then, to resemble the expected $c_r = 0.266c_{\text{air}}$ and $\rho_r = 25\pi\rho_{\text{air}}r/D$ (cf. Fig. 1), we determine $L = 1.69D$ and $w = 0.03D$. The resultant structure is the one illustrated in Fig. 3(a).

We conduct numerical simulations to validate the omnidirectional enhancement of emission. We use a centered source of various order m, and sweep D/λ values by sweeping frequencies. The D/λ values corresponding to the resonant peaks

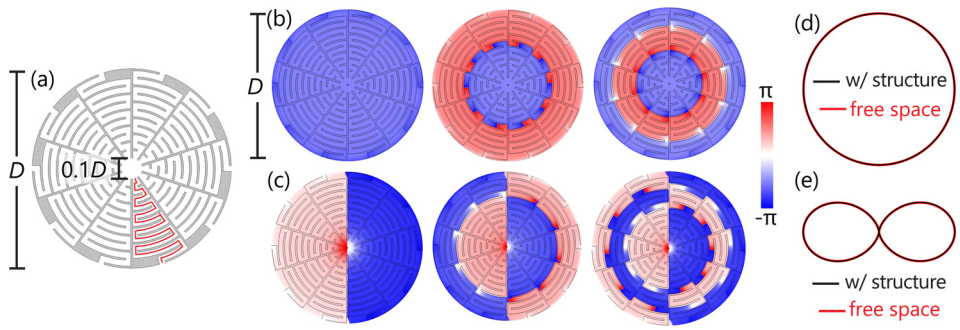

Fig. 3. (Color online) A realistic structure for emission enhancement. (a) The structure is made of rigid materials (gray part), where the coiled air-filled channels elongate the sound path (red line) to reduce the equivalent sound speed c_r along the radial direction and the rigid walls between the channels support the azimuthal anisotropy $\rho_\theta \to \infty$. (b) Phase distribution of sound fields radiated from a monopole source as simulated at three resonant frequencies [cf. Fig. 2(c)]. (c) Same as (b) but for a dipole source. (d,e) Comparison of far-field directivity with and without the enclosure simulated for the lowest resonance in (b) and (c), respectively.

simulated in lossless cases are shown by green circles in Fig. 2(b), which agree well with the results of the conceptual enclosure [black dots in Fig. 2(b)].

The losses would reduce the enhancement near resonances. The amount of reduction depends on the structure size. As an example, for a structure of $D = 10$ cm, numerical simulations with losses included[11] give three peak values of enhancement as $P_1/P_0 = (81, 14, \text{and } 6)$ at $D/\lambda = (0.13, 0.43, \text{and } 0.72)$, in comparison with the lossless case of (267, 52, and 28) at (0.14, 0.44, and 0.73), respectively. The phase distributions of sound fields in the structure at resonances are shown in Figs. 3(b) and 3(c) for monopole and dipole sources, respectively. Even with the losses included, the directivity pattern is still well preserved, as shown in Figs. 3(d) and 3(e) for the cases of monopole and dipole sources, respectively.

5. Discussion

We have presented an extremely anisotropic enclosure in a subwavelength regime for omnidirectionally enhancing emission of monochromatic multipole sources of different orders. Degenerate Mie resonances induced by the extreme anisotropy lead to the emission enhancement at the same low frequencies, which guarantees the subwavelength feature of the enclosure. A structure whose anisotropy and degeneracy were not modeled in prior studies is herein used for achieving the emission enhancement. Our simulations validate that the emission is enhanced at frequencies surrounding the resonant frequencies, while the original directivity is preserved. The results are examined in two-dimensional sound fields, though it is possible to exend to three-dimensional designs.

The resonance-based emission enhancement has apparent disadvantages like the fact that (i) in the region between resonances, the amplitude of the emission relative to that of the source in free space becomes less than one [cf. Fig. 1(c)], and (ii) the amplitude of the resonant peaks decrease by increasing order of the resonances [cf. Figs. 1(c) and 2(a)]. With the degenerate resonances concerned here that do not depend on the multipole order, the emission of a real source composed by different multipoles will be primarily enhanced around the resonances. It would be of interest to extend the enhancement also to broadband sound sources. For that case maybe non-degenerate Mie resonances could be useful.

The concept of enclosing a sound source to enhance the emission could be an analogue of the quantum Purcell effect that modifies the spontaneous emission rate of a quantum source by changing the surrounding environment.[12–16] The enhancement presented here remains to be experimentally verified, and if achieved, would be of broad impacts in various areas where minimized transducers are essential for efficient emission of either omnidirectional or directional sound waves.

Acknowledgments

This work is supported by King Abdullah University of Science and Technology, and by the University of Mississippi through the start-up fund and the 2017 College of Liberal Arts Summer Research Award.

References and links

[1]D. T. Blackstock, *Fundamentals of Physical Acoustics* (John Wiley and Sons, Hoboken, NJ, 2000).
[2]G. Lemaitre, B. Letinturier, and B. Gazengel, "Model and estimation method for predicting the sound radiated by a horn loudspeaker—with application to a car horn," Appl. Acoust. **69**(1), 47–59 (2008).
[3]E. Bängtsson, D. Noreland, and M. Berggren, "Shape optimization of an acoustic horn," Comput. Meth. Appl. Mech. Eng. **192**(11), 1533–1571 (2003).
[4]G. Ballou, *Handbook for Sound Engineers* (Taylor and Francis, Oxford, UK, 2013).
[5]K. Song, S. H. Lee, K. Kim, S. Hur, and J. Kim, "Emission enhancement of sound emitters using an acoustic metamaterial cavity," Sci. Rep. **4**, 4165 (2014).
[6]*Acoustics Module User Guide* [version 4.2] (COMSOL Multiphysics, 2011).
[7]D. A. Bies and C. H. Hansen, *Engineering Noise Control: Theory and Practice* (CRC Press, Boca Raton, FL, 2009).
[8]S. D. Snyder, *Active Noise Control Primer* (Springer, New York, 2012).
[9]Y. Cheng, C. Zhou, B. G. Yuan, D. J. Wu, Q. Wei, and X. J. Liu, "Ultra-sparse metasurface for high reflection of low-frequency sound based on artificial mie resonances," Nat. Mater. **14**(10), 1013–1019 (2015).
[10]X. Zhu, B. Liang, W. Kan, Y. Peng, and J. Cheng, "Deep-subwavelength-scale directional sensing based on highly localized dipolar mie resonances," Phys. Rev. Appl. **5**(5), 054015 (2016).
[11]X. Jiang, Y. Li, and L. Zhang, "Thermoviscous effects on sound transmission through a metasurface of hybrid resonances," J. Acoust. Soc. Am. **141**(4), EL363–EL368 (2017).
[12]J. M. Gérard, B. Sermage, B. Gayral, B. Legrand, E. Costard, and V. Thierry-Mieg, "Enhanced spontaneous emission by quantum boxes in a monolithic optical microcavity," Phys. Rev. Lett. **81**(5), 1110–1113 (1998).

[13]D. Kleppner, "Inhibited spontaneous emission," Phys. Rev. Lett. **47**(4), 233–236 (1981).
[14]P. Goy, J. Raimond, M. Gross, and S. Haroche, "Observation of cavity-enhanced single-atom spontaneous emission," Phys. Rev. Lett. **50**(24), 1903–1906 (1983).
[15]H. N. Krishnamoorthy, Z. Jacob, E. Narimanov, I. Kretzschmar, and V. M. Menon, "Topological transitions in metamaterials," Science **336**(6078), 205–209 (2012).
[16]E. Yablonovitch, "Inhibited spontaneous emission in solid-state physics and electronics," Phys. Rev. Lett. **58**(20), 2059–2062 (1987).